Autophagy inhibitor Lys05 has single-agent antitumor activity and reproduces the phenotype of a genetic autophagy deficiency

Quentin McAfee[a], Zhihui Zhang[b], Arabinda Samanta[a], Samuel M. Levi[b], Xiao-Hong Ma[a], Shengfu Piao[a], John P. Lynch[a], Takeshi Uehara[c], Antonia R. Sepulveda[c], Lisa E. Davis[d], Jeffrey D. Winkler[b,e,1], and Ravi K. Amaravadi[a,e,1]

Departments of [a]Medicine and [c]Pathology, Perelman School of Medicine, [b]Department of Chemistry, School of Arts and Sciences, and [e]Abramson Cancer Center, University of Pennsylvania, Philadelphia, PA 19104; and [d]Department of Pharmacy Practice & Pharmacy Administration, Philadelphia College of Pharmacy, University of the Sciences, Philadelphia, PA 19104

Edited by Dennis A. Carson, University of California at San Diego, La Jolla, CA, and approved April 10, 2012 (received for review November 9, 2011)

Autophagy is a lysosome-dependent degradative process that protects cancer cells from multiple stresses. In preclinical models, autophagy inhibition with chloroquine (CQ) derivatives augments the efficacy of many anticancer therapies, but CQ has limited activity as a single agent. Clinical trials are underway combining anticancer agents with hydroxychloroquine (HCQ), but concentrations of HCQ required to inhibit autophagy are not consistently achievable in the clinic. We report the synthesis and characterization of bisaminoquinoline autophagy inhibitors that potently inhibit autophagy and impair tumor growth in vivo. The structural motifs that are necessary for improved autophagy inhibition compared with CQ include the presence of two aminoquinoline rings and a triamine linker and C-7 chlorine. The lead compound, Lys01, is a 10-fold more potent autophagy inhibitor than HCQ. Compared with HCQ, Lys05, a water-soluble salt of Lys01, more potently accumulates within and deacidifies the lysosome, resulting in impaired autophagy and tumor growth. At the highest dose administered, some mice develop Paneth cell dysfunction that resembles the intestinal phenotype of mice and humans with genetic defects in the autophagy gene *ATG16L1*, providing in vivo evidence that Lys05 targets autophagy. Unlike HCQ, significant single-agent antitumor activity is observed without toxicity in mice treated with lower doses of Lys05, establishing the therapeutic potential of this compound in cancer.

cell death | stress responses | cancer cell survival | drug resistance | antimalarials

Autophagy, the sequestration of organelles and proteins in autophagic vesicles (AVs) and degradation of this cargo through lysosomal fusion (1), allows tumor cells to survive metabolic and therapeutic stresses (2–5). Therapy-induced autophagy is a key resistance mechanism to many anticancer agents (6), and autophagy levels are increased in most cancers (7). Chloroquine (CQ; Fig. 1, compound **1**) derivatives block autophagy by impairing lysosomal function (3, 8, 9). Studies in multiple mouse models of malignancy have demonstrated that autophagy inhibition with CQ derivatives augments the efficacy of a variety of anticancer agents. Clinical trials combining cancer therapies with hydroxychloroquine (HCQ; Fig. 1), have been launched, and preliminary results indicate these combinations have activity (6). However, pharmacokinetic (PK)-pharmacodynamic (PD) studies conducted in patients receiving HCQ for cancer therapy have indicated that the high micromolar concentrations of HCQ required to inhibit autophagy in vitro are inconsistently achieved in humans (10). There is an unmet need to develop more potent inhibitors of autophagy.

The design and synthesis of dimeric analogs of CQ that exploit the thermodynamic advantages imparted by polyvalency (11, 12) has been previously studied in the context of malaria (13–15). The synthesis of heteroalkane-bridged bisquinolines did not produce sufficient antimalarial activity to warrant further investigation (14). Subsequently, a series of tetraquinolines was reported with potent antimalarial properties (13), confirming that polyvalency could afford increased potency. Augmented cytotoxicity was observed in cancer cell lines when Akt inhibitors were combined with fluorinated quinolines (16), and CQ analogs with a piperazine connector had enhanced anticancer properties compared with CQ (17). These results suggest that the CQ scaffold could serve as the basis for the development of effective cancer chemotherapeutics, but to date the properties of dimeric CQ derivatives as anticancer therapeutics have not been investigated. Here we report the synthesis of dimeric CQ analogs and a structure-activity analysis using autophagy and cytotoxicity assays as the biological reporters of activity. This work identifies Lys01 as a viable lead compound for development as an autophagy inhibitor and anticancer therapeutic.

Results

Strategy for Synthesis of Bivalent Aminoquinoline Autophagy Inhibitors. To apply the strategy of polyvalency (11, 12) to the synthesis of autophagy inhibitors, dimeric CQ (Fig. 1; **3**: Lys01) was prepared from commercially available materials (compounds herein are listed in Table S1). Based on literature precedent (14), we envisioned the preparation of **3** from two equivalents of **4** (14) and one equivalent of **5**, as outlined in Fig. S1. Though **6** (R = H) is known (14), the bisquinoline **3** (R = Me) has not been described in the literature. Because of its putative lysosomotropism, we refer to **3** as Lys01 (Fig. 1). Reaction of two equivalents of **4** with **5** led to the formation of a mixture of the desired product **3** along with some of the monoquinoline **7**: Lys02 (Fig. 1 and Fig. S1), the synthesis of which was previously reported (18). To examine the role of the C-7 chlorine substituent in **3**, we prepared **9** (Fig. 1; **9**: Lys-03), the dimethoxy analog of compound **3**, starting from 4-bromo-7-methoxyquinoline **8**. To determine the importance of the polyamine connector of **3**, we prepared the polyether analog **11**: Lys04 of compound **3** from two equivalents of **8** and the commercially available 2,2′-(ethylenedioxy)bis(ethylamine) **10** (Fig. 2).

Lys01 Is a More Potent Autophagy Inhibitor than HCQ or CQ. LN229 (glioblastoma) cells were treated with Lys01 and derivatives Lys02, Lys03, Lys04, HCQ, and CQ. Near complete cell death of cultured cells was observed in cells treated with Lys01 at con-

Author contributions: Q.M., Z.Z., T.U., A.R.S., L.E.D., J.D.W., and R.K.A. designed research; Q.M., Z.Z., A.S., S.M.L., X.-H.M., S.P., J.P.L., T.U., A.R.S., L.E.D., J.D.W., and R.K.A. performed research; Z.Z., S.M.L., J.P.L., T.U., A.R.S., L.E.D., J.D.W., and R.K.A. contributed new reagents/analytic tools; Q.M., A.S., S.M.L., X.-H.M., S.P., J.P.L., T.U., A.R.S., L.E.D., J.D.W., and R.K.A. analyzed data; and Q.M., J.P.L., A.R.S., L.E.D., J.D.W., and R.K.A. wrote the paper.

Conflict of interest statement: There is a patent pending that protects the compounds described in this paper and use of the compounds in cancer and other indications. This patent has not been licensed and has generated no revenue to date.

This article is a PNAS Direct Submission.

[1]To whom correspondence may be addressed. E-mail: ravi.amaravadi@uphs.upenn.edu or winkler@sas.upenn.edu.

This article contains supporting information online at www.pnas.org/lookup/suppl/doi:10.1073/pnas.1118193109/-/DCSupplemental.

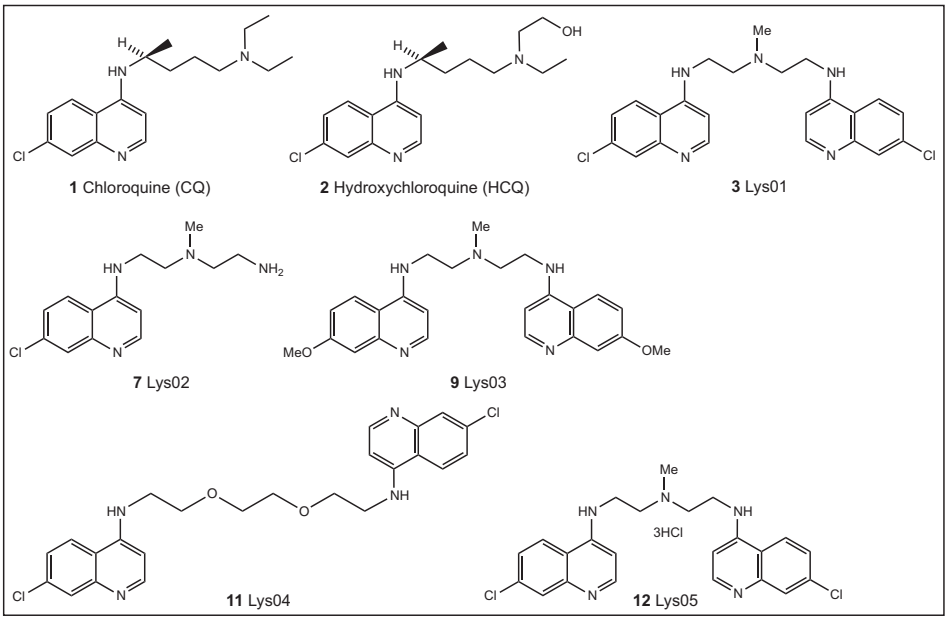

Fig. 1. Chemical structure of mono- and bisaminoquinolines.

centrations of 10 μM or higher between 4 and 24 h. LC3 is a ubiquitin-like protein that exists as an unconjugated form (LC3I) or conjugated to AV membranes (LC3II) (19). An increase in the ratio of LC3II to LC3I reflects the accumulation of AV in cells, and therefore effective autophagy inhibition. LC3 immunoblotting (Fig. 2) demonstrated that Lys01 is a >10-fold more potent autophagy inhibitor than HCQ or CQ at a concentration of 10 μM. Lys02 and Lys03 produced dose–response relationships for LC3 immunoblotting similar to HCQ or CQ, whereas Lys04, which retains the two chloroquinoline rings present in Lys01, demonstrated intermediate potency in the LC3 autophagy assay.

To further characterize the effects of Lys01 on autophagy, LN229 GFP-LC3 cells were treated with Lys01 or HCQ (Fig. 3*A*). Within 4 h of treatment in cells treated with HCQ 1 μM, punctate fluorescence, indicating an accumulation of ineffective AVs, was observed in a minority of cells. HCQ 10 μM produced numerous small puncta, and HCQ 100 μM resulted in larger dense puncta that represent fusion of accumulated AVs. Lys01 1 μM produced numerous small puncta, whereas in Lys01 10 μM produced dense puncta similar to HCQ 100 μM. All cells treated with Lys01 100 μM were dead by 4 h. A significant fivefold increase in GFP-LC3 puncta between 10 μM Lys01 compared with 10 μM HCQ treatments was observed. The average number of vesicles per cell in cells treated with Lys01 10 μM was higher than in cells treated with 100 μM HCQ (Fig. 3*A*). Electron micrographs of LN229 GFP-LC3 cells treated with DMSO, HCQ, or Lys01 further characterized the significant morphological difference in the size and number of vesicles produced by blockade of autophagy with these agents (Fig. 3*B*). Thus, Lys01 produces morphological changes more pronounced than HCQ, at 10-fold lower concentrations. To determine if Lys01 treatment was inducing production of new AVs (an autophagy inducer) or blocking the clearance of AVs (an autophagy inhibitor), a bafilomycin clamp experiment was performed (Fig. 3*C*). LN229 GFP-LC3 cells were treated with DMSO, rapamycin, HCQ, or Lys01 in the absence or presence of bafilomycin. At 24 h, rapamycin treatment resulted in a further increase in the LC3II/LC3 ratio in bafilomycin-treated cells compared with control cells, whereas HCQ- or Lys05-treated cells did not demonstrate an increase in LC3II/LC3I ratio in bafilomycin-treated cells compared with control, confirming that Lys01 is an autophagy inhibitor (Fig. 3*C*).

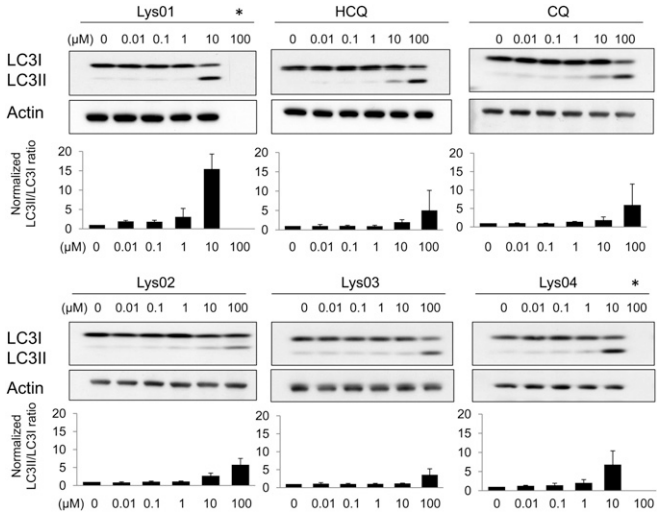

Fig. 2. Effects of Lys01–Lys04 on LC3 immunoblotting. Immunoblotting and quantification of LC3II/LC3I ratio in lysates from LN229 cells treated for 4 h. The graphs show (mean ± SD) LC3II/LC3I ratios of each treatment normalized to the LC3II/LC3I ratio of control-treated cells for each experiment.

To determine the implications of more potent autophagy inhibition on cytotoxicity, LN229 (glioma), 1205Lu (melanoma), HT-29 (colon), and c8161 (melanoma) cells were treated with Lys01, Lys02, Lys03, Lys04, and HCQ at concentrations between 0.01 and 100 μM (Fig. 3*D*). A 3-(4,5-dimethylthiazol-2-yl)-2,5-diphenyltetrazolium bromide (MTT) assay was used to assess viable cells at 72 h. In the four cell lines tested, the IC_{50} of Lys01 was 4–8 μM (Table S2). Near complete cell death after 24 h was observed in 1205Lu and HCC827 cells (cell lines that are highly resistant to HCQ) treated with 10 μM Lys01. In contrast, the IC_{50} for Lys02 (35–91 μM), Lys03 (24–53 μM), and HCQ (15–42 μM) were collectively nine- to 30-fold less potent than Lys01. Lys04 had intermediate activity, with an IC_{50} of 10–17 μM. These studies demonstrate that Lys01 is consistently more cytotoxic than other aminoquinolines tested, or HCQ. Together with the LC3 Western blot data, these results indicate that the most potent cytotoxic autophagy inhibitors contain two aminoquinoline

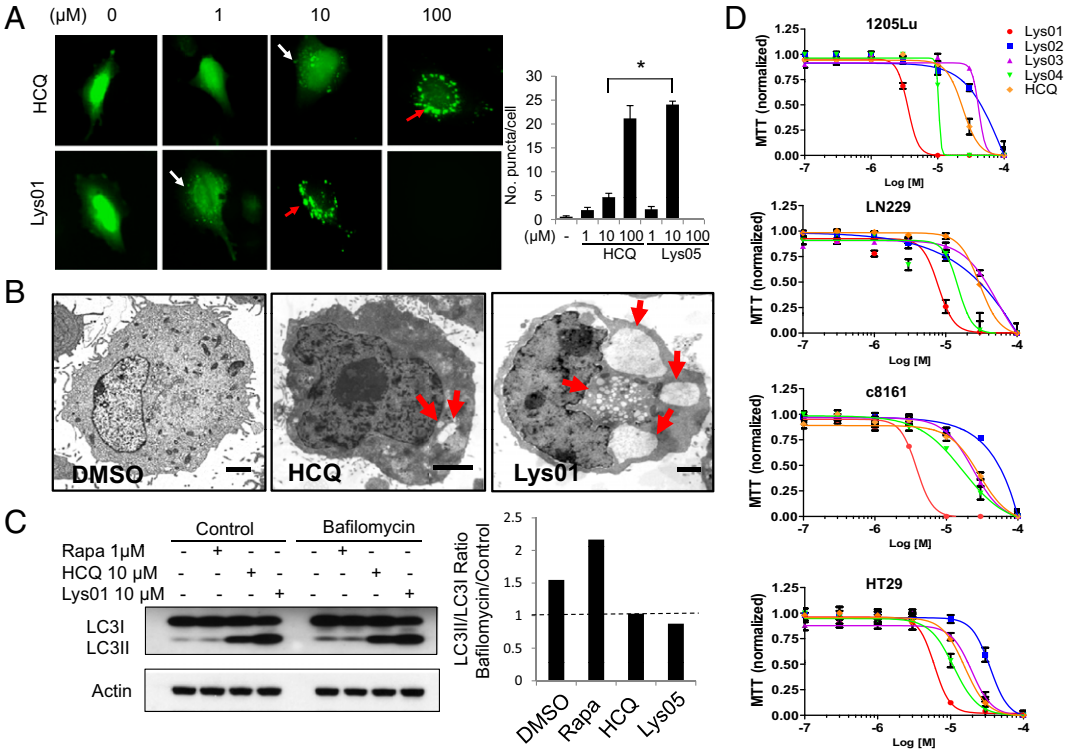

Fig. 3. Autophagy inhibition and cytotoxicity of Lys01 compared with HCQ. (*A*) Representative images of LN229 GFP-LC3 cells treated as indicated for 4 h. White arrows: small puncta; red arrows: dense puncta. Graph shows mean ± SEM puncta per cell. (*B*) Representative electron micrographs of LN229-GFP-LC3 cells treated (4 h) with DMSO, HCQ 10 μM, or Lys01 10 μM. Arrows: autophagic vesicles. (*C*) (*Left*) LC3 immunoblotting of LN229 cells treated for 24 h as indicated. (*Right*) Calculated ratio of LC3II/LC3I ratios for bafilomycin vs. control cotreatment. Ratios higher than 1 (dashed line) indicate an autophagy inducer or control; ratios lower than 1 indicate an autophagy inhibitor. (*D*) MTT assay (72 h) for four cell lines. Red: Lys01; blue: Lys02; purple: Lys03; green: Lys04; orange: HCQ. Values presented are means ± SEM with five replicates per treatment.

rings, the triamine linker present in Lys01 and a chlorine substituent at the C-7 position of the aminoquinoline ring.

In Vivo Autophagy Inhibition and Antitumor Efficacy of Lys05. Lys05, the trihydrochloride salt of Lys01, was synthesized to enhance aqueous solubility and to enable in vivo studies. Lys01 and Lys05 produced equivalent dose-dependent increases in the LC3II/LC3I ratio, accumulation of the autophagy cargo protein p62 (20), and identical IC_{50} values in the MTT assay (Fig. S2 *A* and *B*). To investigate the safety of Lys05 and its in vivo effects on autophagy, c8161 xenografts matched for tumor size were treated with i.p. daily PBS, or equimolar doses of HCQ or Lys05 [HCQ 60 mg/kg (138 nmols/g), Lys05 76 mg/kg (138 nmols/g)] for 48 h. With this high-dose, short-term treatment, no mice died, but after 2 d of dosing, mice treated with Lys05 76 mg/kg i.p. were observed to have arched backs and lethargy. After 48 h of treatment, mice were euthanized, and tumors were processed for EM. Morphologically, EM showed that cells with intact nuclear and cytoplasmic membranes contained large AVs in Lys05-treated tumors (Fig. 4*A*). Quantification of the mean number of AV per cell in two representative tumors from each treatment group found a significant (>twofold) increase in the mean number of AV per cell in Lys05-treated tumors compared with control- or HCQ-treated tumors (Fig. 4*B*). Significantly higher LC3II/LC3I levels were observed in Lys05-treated tumors compared with control- or HCQ-treated tumors, providing further evidence of in vivo autophagy inhibition (Fig. S3*A*). After 48 h of treatment, cleaved caspase 3 levels indicative of apoptosis were elevated in Lys05-treated tumors compared with HCQ- or PBS-treated tumors.

Except for certain models of pancreatic cancer (21), in many animal tumor models, where high levels of autophagy are likely present in untreated tumors (4, 22), treatment with single-agent HCQ does not impair tumor growth (23, 24). To determine if a more potent autophagy inhibitor such as Lys05 could significantly impair tumor growth as a single agent, 1205Lu xenografts were generated in the flanks of nude mice. For chronic treatment experiments, the 1205Lu melanoma model was chosen over the c8161 xenograft model because c8161 xenografts tend to spontaneously ulcerate, confounding tumor measurements and safety analysis. Ten mice bearing 1205Lu xenografts matched for tumor volume per cohort were assigned to PBS, HCQ 60 mg/kg i.p., or Lys05 76 mg/kg i.p. and dosed for 3 d of daily treatment with 2 d off treatment (3/5 d) for all three treatment groups, to allow for symptom recovery and avoid excess toxicity. This schedule was tolerated well for a 14-d period. Tumor growth was significantly impaired in Lys05-treated tumors compared with controls (Fig. 4*C*). Lys05 treatment resulted in a 53% reduction in the average daily tumor growth rate compared with vehicle-treated controls (31.2 vs. 14.6 mm^3/d; $P = 0.002$; Fig. 4*D*). A significant three- and sixfold accumulation of AV was observed at the end of 14 d of treatment in HCQ- and Lys05-treated tumors, respectively, compared with control-treated tumors (Fig. S3*B*). Extensive tumor necrosis was observed in Lys05-treated tumors (Fig. S3*B*).

To determine if lower doses of Lys05 could produce antitumor activity, mice bearing HT-29 colon cancer xenografts were treated with PBS, or Lys05 at 10 mg/kg i.p. daily, 40 mg/kg i.p. daily, or 80 mg/kg i.p. 3/5 d. Clinical toxicity was observed only in the 80 mg/kg cohort, with 2/8 mice euthanized early for bowel obstruction. Daily dosing for the 10 mg/kg and 40 mg/kg cohorts was well tolerated. The average daily tumor growth rate was significantly impaired in a dose-dependent fashion with Lys05 treatment (Fig. 4*E*). Tumor growth curves demonstrated that all three doses of Lys05 produced significant tumor growth impairment compared with control (Fig. 4*F*). Excised tumor weights demonstrated that significant antitumor activity was observed with 10 mg/kg daily dosing (Fig. 4*G*). Immunoblotting against LC3 in tumor lysates harvested after 14 d of treatment revealed a significant increase in LC3II/

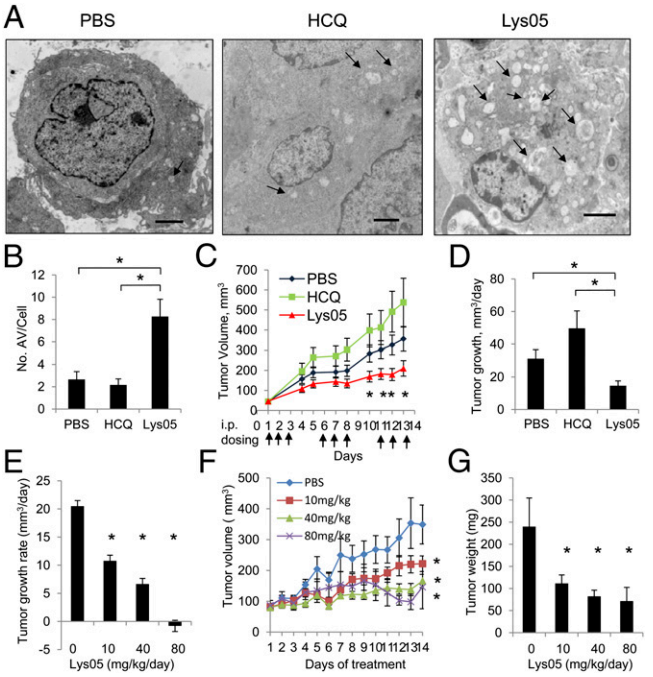

Fig. 4. In vivo autophagy inhibition and antitumor activity of Lys05. (*A*) Representative electron micrographs (12,000×) of c8161 xenograft tumors harvested after 2 d of daily i.p. treatment with PBS, HCQ 60 mg/kg, or Lys05 76 mg/kg. Arrows: autophagic vesicles. (Scale bar: 2 μm.) (*B*) Quantification of mean ± SEM number of autophagic vesicles per cell from two representative tumors from each treatment group. (*C* and *D*) 1205Lu xenografts were treated with PBS (blue), HCQ 60 mg/kg i.p. (green), or Lys05 76 mg/kg (red) i.p. every 3/5 d. (*C*) Tumor volumes over 14 d. (*D*) Daily tumor growth rate. (*E*–*G*) HT29 xenografts were generated in the flanks of nude mice and treated with PBS, Lys05 10 mg/kg i.p. daily, Lys05 40 mg/kg i.p. daily, or Lys05 80 mg/kg i.p. every 3/5 d. (*E*) Average daily tumor growth rate. (*F*) Tumor volumes over 14 d. (*G*) Weight of excised tumors, $^*P < 0.05$.

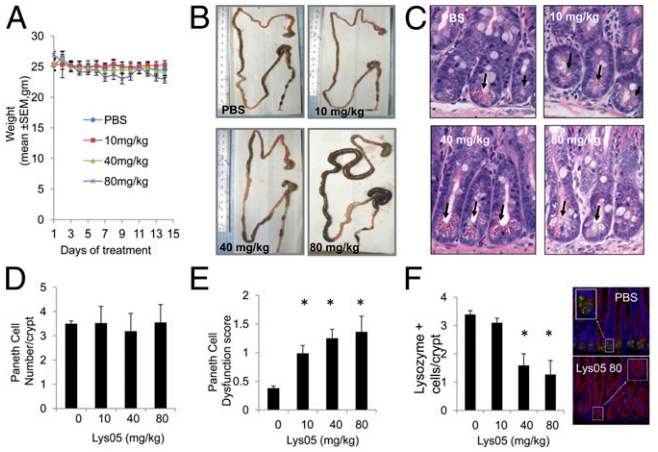

Fig. 5. Lys05 treatment at the highest dose reproduces the intestinal phenotype of a genetic autophagy deficiency. (*A*–*F*) Weight and intestines were analyzed for mice bearing HT29 xenografts treated with PBS and Lys05 10–80 mg/kg. (*A*) Daily weight. (*B*) Representative excised gastrointestinal tracts after 14 d of treatment. (*C*) Representative images (40×) of H&E-stained ileal crypts from mice bearing HT29 xenografts (14 d). Arrows: Paneth cells. (*D*) Paneth cell number per crypt. (*E*) Paneth cell dysfunction score, $^*P < 0.05$. (*F*) Scoring of lysozyme-positive cells, $^*P = 0.001$. Representative images of lysozyme immunofluorescence (green) of ileum in mice treated with PBS and Lys05 80 mg/kg i.p. 3/5 d.

LC3I ratio in all Lys05-treated tumors, including the 10 mg/kg-dosed tumors compared with control (Fig. S3*C*).

Intestinal Toxicity at the Maximal Administered Dose of Lys05 Resembles a Genetic Autophagy Deficiency. In the 1205Lu xenograft experiment, individual animals treated with Lys05 76 mg/kg i.p. 3/5 d appeared lethargic with arched backs (Fig. S4*A*). Three of 10 mice treated with Lys05 developed bowel obstruction (Fig. S4*B*). Inspection of the bowel found dilated proximal small intestine with a pseudostricture of the terminal ileum. Histological examination of the ileum revealed no evidence of excess inflammation, fibrosis, or mechanical obstruction, indicating that the obstructive signs observed in the mice were due to pseudo-obstruction or functional ileus. Though intestinal villi and crypt architecture were intact, dysmorphic Paneth cells (Fig. S4*C*) were observed. Paneth cell dysfunction, including reduced size and number of eosinophilic lysozyme-containing granules, has previously been described as the pathognomonic sign of autophagy deficiency in mice and a subset of Crohn disease patients that have a genetic deficiency in the essential autophagy gene *ATG16L1* (25).

In the HT29 dose-finding xenograft experiment there was no significant weight loss observed (Fig. 5*A*). Resection of the entire gastrointestinal tract from mice bearing HT-29 tumors after 14 d of treatment demonstrated bowel thickening and obstruction was limited to the 80-mg/kg dose cohort (Fig. 5*B*). Histological examination of the terminal ileum resected from mice bearing HT-29 xenografts demonstrated dose-dependent effects on Paneth cell morphology (Fig. 5*C*). Though the number of Paneth cells per crypt did not change with treatment (Fig. 5*D*), the size and number of granules decreased in a dose-dependent manner. Scoring on a Paneth cell dysfunction scale (*Materials and Methods* and Fig. S5) indicated that Paneth cell dysfunction was observed at all doses tested of Lys05, but toxicity was restricted to the 80-mg/kg dose (Fig. 5*E*). In mice treated with Lys05 40 mg/kg or 80 mg/kg, but not 10 mg/kg, lysozyme was significantly reduced or absent in Paneth cells (Fig. 5*F*). Taken together, these findings indicate that Lys05-associated Paneth cell dysfunction mimics *ATG16L1* deficiency, and lower doses of Lys05 produce significant antitumor activity without dose-limiting toxicity.

Lys05 Inhibits Autophagy by Deacidifying the Lysosome. To compare the relative lysosomal accumulation of Lys05 and HCQ, lysosomes were subfractionated from 1205Lu cells treated with PBS, HCQ 10 μM, or Lys05 10 μM, and 1205Lu tumors harvested after 14 d of treatment with PBS, HCQ 60 mg/kg i.p., or Lys05 76 mg/kg i.p. every 3/5 d. Immunoblotting against the lysosomal marker LAMP2 confirmed adequate separation of the lysosomal and whole-cell population in cells and tumor samples (Fig. 6*A*). HPLC tandem mass spectrometry measurements (Fig. S6) determined that the concentrations of Lys05 and HCQ in the whole-cell homogenate treated with Lys05 10 μM or HCQ 10 μM for 24 h were 57 μM and 8 μM, respectively, indicating a sixfold-higher concentration of Lys05 within the cell compared with HCQ. The concentration of Lys05 and HCQ in the lysosomal fraction of cells treated with Lys05 10 μM or HCQ 10 μM were 105 μM and 13 μM, respectively, indicating an eightfold-higher concentration of Lys05 in the lysosome compared with HCQ. This difference in cellular and lysosomal accumulation of Lys05 and HCQ was more marked in tumor tissue. There was an 11-fold-higher concentration and a 34-fold-higher concentration of Lys05 compared with HCQ in whole-cell homogenates and lysosomes, respectively, within tumors (Fig. 6*B*).

Having established that Lys05 more effectively accumulates in the lysosome than HCQ, the functional effects of this accumulation were investigated. 1205Lu cells were treated with vehicle, Lys05, and HCQ, and stained with LysoTracker Red (Fig. 6*C*). Within 30 min of treatment, fewer LysoTracker-positive puncta were observed in Lys05-treated cells at both 10 μM and 100 μM concentrations. In contrast, a significant decrease in LysoTracker-positive puncta was observed in cells treated with HCQ 100 μM, but not observed in cells treated with HCQ 10 μM. Next, 1205Lu cells were treated with vehicle, Lys05, or HCQ and stained with acridine orange (AO; a dye that aggregates in all endovesicular acidic compartments) at 24 h (Fig. 6*D*). HCQ produced a dose-

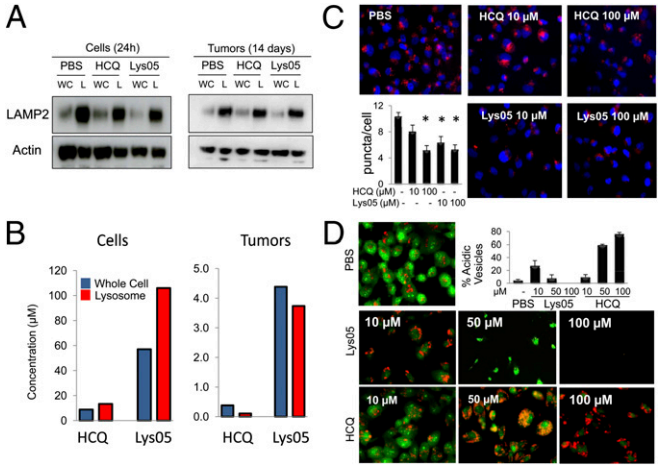

Fig. 6. Lys05 inhibits autophagy by accumulating in and deacidifying the lysosome. (*A*) 1205Lu cells (treated with PBS, HCQ 10 μM, or Lys05 10 μM for 24 h) and harvested 1205Lu xenograft tumors (treated with PBS, HCQ 60 mg/kg i.p. 3/5 d, or Lys05 76 mg/kg i.p. 3/5 d for 14 d) were homogenized and fractionated into whole-cell (WC) and lysosomal (L) fractions. LAMP2 immunoblotting confirmed isolation of concentrated lysosomes for analysis. (*B*) Concentrations of HCQ or Lys05 in cells and tumor WC and L homogenates. (*C*) Fluorescence imaging of 1205Lu cells treated as indicated for 30 min and stained with LysoTracker Red. LysoTracker puncta (red) per cell was scored for three high-powered fields. Blue: nuclear DAPI staining. Data presented is mean ± SEM. (*D*) Fluorescence imaging of c8161 cells treated as indicated for 24 h and stained with AO. Orange: aggregated AO; green: diffuse AO. Graph shows mean +/− SD %acidic vesicles.

dependent accumulation of acidic vesicles. In contrast, Lys05 caused an accumulation of acidic vesicles at lower doses (10 μM), but at higher doses (50 μM), no acidic vesicles were observed, indicating the complete deacidification of the endovesicular system.

Finally, the functional consequences of lysosomal deacidification were investigated by measuring enzymatic activity of acid phosphatase. In 1205Lu cells treated with PBS, HCQ 10 μM, or Lys05 10 μM, within 24 h there was a 43% reduction in acid phosphatase activity in the lysosomal fraction of Lys05-treated vs. PBS-treated cells (Fig. S7*A*). Leakage of certain lysosomal enzymes, such as activated cathepsins, could lead to an autophagy-independent cell death. Within 24 h of treatment of 1205Lu cells with PBS, HCQ, or Lys05, there was decreased acid-dependent processing of immature cathepsin D to the mature activated form within the lysosome in Lys05-treated compared with HCQ- or PBS-treated cells (Fig. S7*B*), In 1205Lu xenograft tumors, after 14 d of treatment there was a 1.75-fold increase in extralysosomal acid phosphatase activity in the Lys05-treated tumors, suggesting that chronic treatment can lead to extralysosomal leakage of enzymes (Fig. S7*C*), but increased acid-dependent processing of cathepsin D within the whole-cell homogenate was not observed in Lys05-treated tumors (Fig. S7*D*). These results indicate that high doses of Lys05 cause lysosomal dysfunction by deacidifying the lysosome, leading to impairment of lysosomal enzymes and effective autophagy inhibition, whereas high doses of HCQ incompletely deacidify the lysosome, leading to incomplete autophagy inhibition associated with less cell death.

Discussion

Polyvalent molecules can have properties that differ significantly from those of the corresponding monomers (11, 12). The rationale for the development of dimeric species as pharmaceuticals derives from the possible binding of the dimeric ligand at two distinct binding sites either on a single receptor or at defined sites on two separate monomers of a dimeric protein (26). We have designed Lys01 as a dimeric form of CQ, with the spacer *N,N*-bis(2-aminoethyl)methylamine **5** as the connector between two CQ moieties. The preliminary structure-activity relationship (SAR) that emerges from these studies indicates that the bivalent quinoline structure of Lys01 is critical to the observed biological activity, because the monomeric compound Lys02 is a much less potent autophagy inhibitor. Our results also indicate the importance of both the 7-chloro substituent and the bisaminoethyl–methylamine linker in Lys01, because the corresponding bismethyl ether Lys03, with the same bisaminoethyl–methylamine linker present in Lys01, is not as potent as Lys01. Lys04, which contains the 7-chloroquinoline rings present in Lys01, but contains a polyether linkage in place of the triamino linkage present in Lys01 and Lys03, is also not as potent as Lys01. Lys01 and its trihydrochloride salt Lys05 were not only more potent at blocking autophagy in vitro, but also produced cytotoxicity in multiple cancer cell lines and antitumor activity in multiple human tumor xenograft models.

The significant 3- to 10-fold difference between Lys05 and HCQ in lysosomal concentration, autophagy inhibition, and cytotoxicity observed with Lys01 compared with HCQ, cannot be attributed to a simple concentration effect, i.e., doubling of the concentration of the quinolone ring in Lys01. However, the enhanced basicity of the pentaamino structure of Lys01 compared with the structures of both CQ and HCQ, each of which contain only three nitrogen atoms, could lead to enhanced sequestration of Lys01 in the acidic lysosome relative to that of CQ and HCQ, respectively. Another possible basis for the difference in potency between the monomeric aminoquinolines and the bisquinoline autophagy inhibitor Lys01 is that bivalency could facilitate cooperative inhibition of an unknown lysosomal protein target, or lead to decreased affinity for drug efflux pumps such as ATP-binding cassette transporters. Our previous work demonstrated that pharmacological inhibition with CQ produces the equivalent antitumor effect as knockdown of an essential autophagy gene *ATG5*, establishing that the CQ derivatives act as autophagy inhibitors when dosed at low micromolar doses (3). In this study, we have demonstrated that Lys01 produces more complete lysosomal deacidification and autophagy inhibition than HCQ. The difference in the magnitude of lysosomal inhibition that can be achieved with Lys05 compared with HCQ in vivo is evidenced by the 34-fold-higher concentrations of Lys05 in tumor lysosomes compared with HCQ and the associated doubling of AV accumulation associated with Lys05 compared with HCQ treatment in 1205Lu xenografts. Incomplete deacidification of the lysosome could result in rebound increase in endovesicular acidity and autophagic capacity. These findings may explain why intermittent single-agent Lys05 had significant antitumor activity, whereas intermittent HCQ treatment resulted in acceleration of tumor growth in 1205Lu xenografts. Others have demonstrated that, during effective distal autophagy inhibition, accumulation of dysfunctional AV and eventual bursting of lysosomes (27, 28) conspire to increase reactive oxygen species, generating DNA damage, followed by cell death by apoptosis or necrosis (21). Our data support the mechanism of action of lysosomal impairment for Lys01, but identification of a molecular target within the lysosome for Lys01 will be the focus of future research.

The Paneth cell dysfunction observed at the highest dose of Lys05 administered supports the proposed mechanism of action of the drug. Paneth cells are secretory cells of the gut that are responsible for protection against bacterial overgrowth. Proper expression and secretion of a key antibacterial enzyme lysozyme likely requires functional autophagy. Recent evidence supports a critical role for autophagy in the processing of secreted proteins (29). The sensitivity of Paneth cells to high doses of Lys05 suggests that Paneth cell dysfunction could accompany other novel autophagy inhibitors that are currently under development. Patients treated with high doses of HCQ also complain of constipation and nausea.* In mice treated with lower doses of Lys05, chronic daily dosing was associated with some

*Algazy KM, et al. (2011) Combined mTOR inhibition and autophagy inhibition: Phase I trial of temsirolimus and hydroxychloroquine in patients with advanced solid tumors. One Hundred Second Annual Meeting of the American Association for Cancer Research, April 2–6, 2011, Orlando, FL, abstr 4500.

degree of Paneth cell dysfunction but no clinical signs of gastrointestinal toxicity. These findings indicate that Lys01 is a lead compound with great potential to be optimized further for potency as an autophagy inhibitor. Because autophagy inhibitors will likely be incorporated into combination regimens involving one or more anticancer therapies, the antitumor activity observed with low doses and intermittent dosing bodes well for the development of Lys01 and its derivatives as cancer therapeutics. Finally, the enhanced lysosomal accumulation, autophagy inhibition, and therapeutic activity observed with this bisaminoquinoline in cancer models suggest that quinoline polyvalency may also be associated with improved therapeutic activity in diseases such as malaria and rheumatic disorders, in which CQ derivatives have played an important therapeutic role for decades.

Materials and Methods

Chemical Synthesis of Compounds Lys01–Lys05. See *SI Materials and Methods*.

Cell Lines and Plasmids. Cell lines C8161 and PC-9 were maintained in DMEM, LN229, and 1205Lu in RPMI-1640, and both supplemented with 10% (vol/vol) FBS (Sigma), in an atmosphere of 5% CO^2 at 37 °C. LN229 GFP-LC3 was generated as previously described (22).

Fluorescence Imaging. C8161 GFP-LC3 cells were treated and fixed with 4% (vol/vol) paraformaldehyde. Fluorescence imaging was captured at using a Zeiss wide-field microscope. Twenty-five cells per treatment were scored for GFP-LC3 puncta using ImageJ software. For LysoTracker Red, cells were treated for 30 min and labeled for 15 min with 25 nM LysoTracker Red. For AO, cells were treated for 24 h and stained with 5 μM AO. Digital images were captured using a Zeiss Axioplan 2. Experiments were conducted in triplicates. Scoring of LysoTracker puncta and AO cells was conducted using Adobe Photoshop CS4 Extended.

MTT and Acid Phosphatase Assay. For the MTT assay (Roche) cells were treated in five replicates and analyzed after 72 h per the manufacturer's protocol. The Acid Phsophatase Assay kit (Sigma) was used according to the manufacturer's protocol.

Immunoblotting. Cells were lysed in RIPA buffer with protease inhibitors (Roche) and phosphatase inhibitor (Sigma). Immunoblotting was performed as previously described using the following antibodies: LC3 (QCB Biologicals), P62/SQSTM1 (Santa Cruz), actin (Santa Cruz), LAMP2 (Santa Cruz), and cathepsin D (Santa Cruz). Band densities from Western blots were quantified using Adobe Photoshop CS4 Extended.

Tumor Xenograft Experiments. Approval for animal care and use was provided by the Institutional Animal Care and Use Committee at the University of Pennsylvania. All experiments were carried out using 5- to 8-wk-old *Nu/Nu* nude mice obtained from Charles River Labs. Cultured C8161, 1205Lu, or HT29 cells were harvested and suspended in ice-cold PBS and expanded in vivo by s.c. injection into the left flank of mice ($1–2 \times 10^6$ cells/flank). Tumor size was measured using digital calipers, and tumor volume was calculated using the following formula: volume (mm^3) = 1/2 A (length) × B $(width)^2$. For tumor immunoblotting, tumor tissue manually crushed in 12 vol of RIPA buffer.

Electron Microscopy, Histology, and Immunofluorescence. EM processing scoring of AV was performed as previously described (3, 34). See *SI Materials and Methods* for histological scoring and lysozyme staining.

Lysosomal Subfractionation and HPLC Methods. Cell homogenates were enriched for lysosomal fractions by differential centrifugation followed by density centrifugation (Lysosome Extraction Kit; Sigma-Aldrich). For measurement of Lys05 and HCQ using HPLC MS/MS, see *SI Materials and Methods*.

ACKNOWLEDGMENTS. We thank Dr. Donna Huryn for helpful comments, Daisy Flores for lysozyme immunostaining, and Ray Meade and the biomedical imaging core for help with the microscopy. This work was supported by an Abramson Cancer Center pilot award and National Cancer Institute Grant 1K23CA120862 (to R.K.A.).

1. Lum JJ, DeBerardinis RJ, Thompson CB (2005) Autophagy in metazoans: Cell survival in the land of plenty. *Nat Rev Mol Cell Biol* 6:439–448.
2. Amaravadi RK, Thompson CB (2007) The roles of therapy-induced autophagy and necrosis in cancer treatment. *Clin Cancer Res* 13:7271–7279.
3. Amaravadi RK, et al. (2007) Autophagy inhibition enhances therapy-induced apoptosis in a Myc-induced model of lymphoma. *J Clin Invest* 117:326–336.
4. Degenhardt K, et al. (2006) Autophagy promotes tumor cell survival and restricts necrosis, inflammation, and tumorigenesis. *Cancer Cell* 10:51–64.
5. Amaravadi RK (2008) Autophagy-induced tumor dormancy in ovarian cancer. *J Clin Invest* 118:3837–3840.
6. Amaravadi RK, et al. (2011) Principles and current strategies for targeting autophagy for cancer treatment. *Clin Cancer Res* 17:654–666.
7. Lazova R, et al. (2012) Punctate LC3B expression is a common feature of solid tumors and associated with proliferation, metastasis, and poor outcome. *Clin Cancer Res* 18:370–379.
8. Carew JS, et al. (2007) Targeting autophagy augments the anticancer activity of the histone deacetylase inhibitor SAHA to overcome Bcr-Abl-mediated drug resistance. *Blood* 110:313–322.
9. Degtyarev M, et al. (2008) Akt inhibition promotes autophagy and sensitizes PTEN-null tumors to lysosomotropic agents. *J Cell Biol* 183:101–116.
10. Rosenfeld MR, et al. (2010) Pharmacokinetic analysis and pharmacodynamic evidence of autophagy inhibition in patients with newly diagnosed glioblastoma treated on a phase I trial of hydroxychloroquine in combination with adjuvant temozolomide and radiation (ABTC 0603). *J Clin Oncol*, 28: 15s (abstr).
11. Vance D, Shah M, Joshi A, Kane RS (2008) Polyvalency: A promising strategy for drug design. *Biotechnol Bioeng* 101:429–434.
12. Shrivastava A, Nunn AD, Tweedle MF (2009) Designer peptides: Learning from nature. *Curr Pharm Des* 15:675–681.
13. Girault S, et al. (2001) Antiplasmodial activity and cytotoxicity of bis-, tris-, and tetraquinolines with linear or cyclic amino linkers. *J Med Chem* 44:1658–1665.
14. Vennerstrom JL, et al. (1998) Bisquinolines. 2. Antimalarial *N,N*-bis(7-chloroquinolin-4-yl)heteroalkanediamines. *J Med Chem* 41:4360–4364.
15. Burnett JC, et al. (2003) Novel small molecule inhibitors of botulinum neurotoxin A metalloprotease activity. *Biochem Biophys Res Commun* 310:84–93.
16. Hu C, Raja Solomon V, Cano P, Lee H (2010) A 4-aminoquinoline derivative that markedly sensitizes tumor cell killing by Akt inhibitors with a minimum cytotoxicity to non-cancer cells. *Eur J Med Chem* 45:705–709.
17. Solomon VR, Hu C, Lee H (2010) Design and synthesis of chloroquine analogs with anti-breast cancer property. *Eur J Med Chem* 45:3916–3923.
18. Higuchi T, Omiya H, Umezawa M, Kim HS, Wataya Y (2007) Compound with antimalarial activity and antimalarial drug containing the same as active ingredient. Eur Patent Appl 07737389.2, Publ WO 2007/097450 (30.08.2007 Gazette 2007/35).
19. Tanida I, Ueno T, Kominami E (2004) LC3 conjugation system in mammalian autophagy. *Int J Biochem Cell Biol* 36:2503–2518.
20. Pankiv S, et al. (2007) p62/SQSTM1 binds directly to Atg8/LC3 to facilitate degradation of ubiquitinated protein aggregates by autophagy. *J Biol Chem* 282: 24131–24145.
21. Yang S, et al. (2011) Pancreatic cancers require autophagy for tumor growth. *Genes Dev* 25:717–729.
22. Ma XH, et al. (2011) Measurements of tumor cell autophagy predict invasiveness, resistance to chemotherapy, and survival in melanoma. *Clin Cancer Res* 17:3478–3489.
23. Fan QW, et al. (2010) Akt and autophagy cooperate to promote survival of drug-resistant glioma. *Sci Signal* 3:ra81.
24. Saleem A, et al. (2012) Effect of dual inhibition of apoptosis and autophagy in prostate cancer. *Prostate*, 10.1002/pros.22487.
25. Cadwell K, et al. (2008) A key role for autophagy and the autophagy gene Atg16l1 in mouse and human intestinal Paneth cells. *Nature* 456:259–263.
26. Chow LM, Chan TH (2009) Novel classes of dimer antitumour drug candidates. *Curr Pharm Des* 15:659–674.
27. Boya P, Kroemer G (2008) Lysosomal membrane permeabilization in cell death. *Oncogene* 27:6434–6451.
28. Poole B, Ohkuma S (1981) Effect of weak bases on the intralysosomal pH in mouse peritoneal macrophages. *J Cell Biol* 90:665–669.
29. Manjithaya R, Anjard C, Loomis WF, Subramani S (2010) Unconventional secretion of Pichia pastoris Acb1 is dependent on GRASP protein, peroxisomal functions, and autophagosome formation. *J Cell Biol* 188:537–546.